

Coupling effect analysis between the central nervous system and the CPG network with proprioception

Bin He^{†*}, Qiang Lu^{†,‡} and Zhipeng Wang[†]

[†]College of Electronics and Information Engineering, Tongji University, Shanghai, 201804, China

[‡]College of Information and Engineering, Taishan Medical University, Taian, 271016, China

(Accepted February 20, 2014. First published online: April 1, 2014)

SUMMARY

Human rhythmic movement is generated by central pattern generators (CPGs), and their application to robot control has attracted interest of many scientists. But the coupling relationship between the central nervous system and the CPG network with external inputs is still not unveiled. According to biological experiment results, the CPG network is controlled by the neural system; in other words, the interaction between the central nervous system and the CPG network can control human movement effectively. This paper offers a complex human locomotion model, which illustrates the coupling relationship between the central nervous system and the CPG network with proprioception. Based on Matsuoka's CPG model (K. Matsuoka, *Biol. Cybern.* **52**(6), 367–376 (1985)), the stability and robustness of the CPG network are analyzed with external inputs. In order to simulate the coupling relationship, the Radial Basis Function (RBF) neural network is used to simulate the cerebral cortex, and the Credit-Assignment Cerebellar Model Articulation Controller algorithm is employed to realize the locomotion mode conversion. A seven-link biped robot is chosen to simulate the walking gait. The main discoveries include: (1) the output of a new CPG network, which is stable and robust, can be treated as proprioception. Proprioception provides the central nervous system with the information about all joint angles; (2) analysis on a new locomotion model reveals that the cerebral cortex can modulate CPG parameters, leading to adjustment in walking gait.

KEYWORDS: Central pattern generator (CPG); Proprioception; Central nervous system; CA-CMAC; Human locomotion.

1. Introduction

Through neurophysiological studies of animal locomotion, it has been determined that the basic rhythmic movements are controlled by central pattern generators (CPGs). Due to their simplicity and effectiveness, the Matsuoka CPG model¹ has been widely applied to the robot control and modeling and to the motion simulation of humans.^{2–5} In human locomotion, proprioception also plays an important role in detecting the state of the body and serving as a sensory feedback for underlying neural circuits.

Proprioception is the ability to know where our body is at all times. Kondo *et al.*⁶ showed that the automatic movement was mainly realized at the spinal cord based on proprioceptive feedback. Ehrsson *et al.*⁷ showed that the body was distinguished from other objects by its involvement in the correlation or matching of special patterns of intersensory information. Ehrsson⁸ also demonstrated that multisensory correlations were sufficient to determine the perceived location of one's own body. Overholt *et al.*⁹ treated proprioception as a sense of body position and movement that supported control over many automatic motor functions such as posture and locomotion. Beers *et al.*¹⁰ studied the precision of proprioceptive localization of hand in humans. They demonstrated that proprioception provides the central nervous system with the information about the spatial location of body parts. The

* Corresponding author. E-mail: hebin@tongji.edu.cn

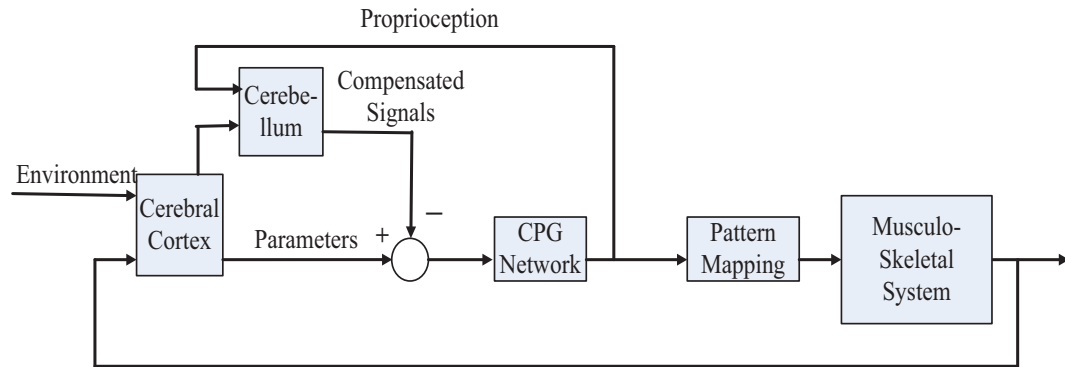


Fig. 1. The locomotion model.

central nervous system needs to know the angles of all joints between the hand and the body so as to combine these angles with known segment lengths to localize a hand. Bartsch *et al.*¹¹ treated the CPG as a proprioception in the locomotion of a humanoid robot.

The central nervous system plays a key role in human locomotion. The accurate movement controlled by neural circuits, such as the walking gait, involves the cerebral cortex and the cerebellum. The basic mechanisms of the locomotion control are located in the spinal cord whose interneurons are involved in the CPG network and pattern formation.^{12,13} Takakusaki and Okumura¹³ demonstrated that the cerebellum could receive massive proprioceptive information and operate as a “comparator” for the control of movements. After comparing and calculating differences between two signals, i.e., the command signal from the cerebral cortex and the sensory feedback from the spinal cord, the cerebellum sends differences to the cerebral cortex and the spinal cord. Therefore, it is an important work to study the coupling relationship between the central nervous system and the CPG network with proprioception in the fields of motor neurology and robot motor control.

This paper is organized as follows. Section 2 presents a new locomotion model and a new CPG network, including the explanation of the model principle and the analysis of the stability and robustness of the CPG network. Section 3 shows the model of the central nervous system. The simulations are given in Section 4. The conclusions and future works are made in Section 5.

2. Locomotion Model and CPG Network Model

2.1. Locomotion model

A new locomotion model selecting the gait as a research object is built on the basis of biological relationship between the locomotion and the central nervous system.¹³ This new model includes the central nervous system and the CPG network, as shown in Fig. 1.

In Fig. 1, the cerebral cortex predicts the CPG network parameter values corresponding to the next gait and sends these to the CPG network and the cerebellum according to environmental change and the current gait. The cerebellum compares the parameter values from the cerebral cortex with those from the CPG network. After calculating the mean square deviation, which is treated as compensation, the cerebellum sends the compensation to the CPG network. Through the mode of conversion, the outputs of the CPG network are changed into the positions and angles, which inspire the musculoskeletal system, and the walking gait is obtained. At the same time, these parameters' values of the CPG network feed back to the cerebellum. In the following seven-link biped robot model, the sensory information is joint angles, which correspond to these CPG outputs. Therefore, the CPG feedbacks are the proprioception in the new model.

In order to explain the locomotion model, a seven-link biped robot model¹⁴ is used to simulate the walking gait, as shown in Fig. 2.

In Fig. 2, each foot trajectory can be denoted by a vector $X_a = [x_a(t), z_a(t), \theta_a(t)]^T$, where $(x_a(t), z_a(t))$ is the coordinate of the ankle position and $\theta_a(t)$ denotes the angle of the ankle. The hip trajectory can be denoted by vector $X_h = [x_h(t), z_h(t), \theta_h(t)]^T$, where $(x_h(t), z_h(t))$ is the coordinate

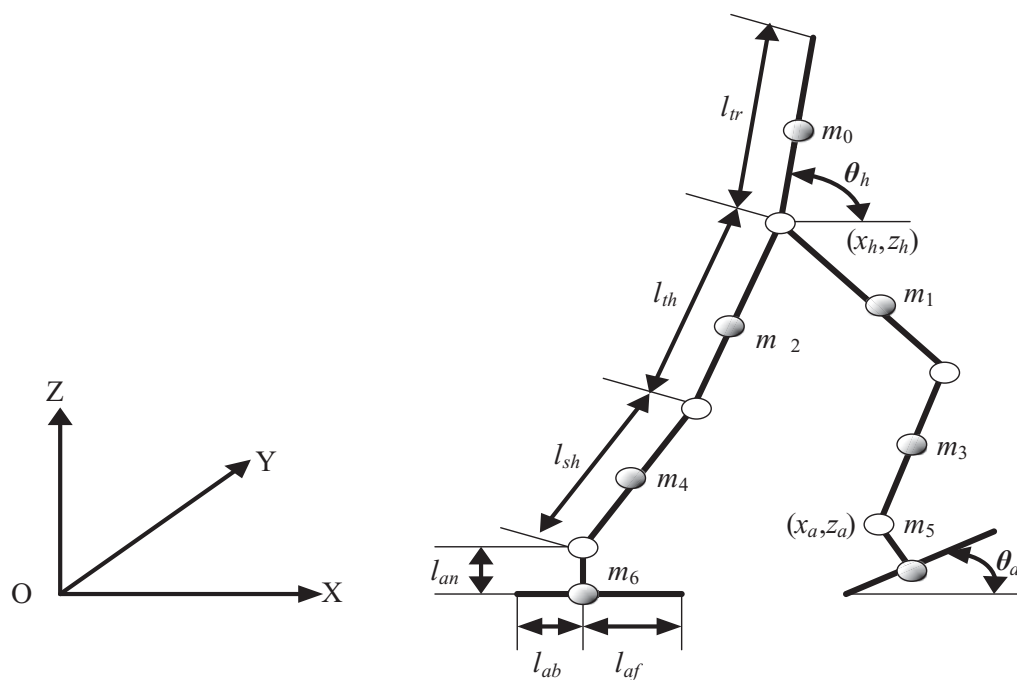


Fig. 2. Model of a biped robot.

of the hip position and $\theta_h(t)$ denotes the hip angle. The parameters are set as $l_{tr} = 50$ cm, $l_{th} = 30$ cm, $l_{sh} = 30$ cm, $l_{an} = 10$ cm, $l_{ab} = 10$ cm, $l_{af} = 13$ cm, $m_0 = 43$ kg, $m_1 = m_2 = 10$ kg, $m_3 = m_4 = 5.7$ kg, and $m_5 = m_6 = 3.3$ kg.¹⁵

2.2. CPG network model

Every joint of the robot is driven by a neural oscillator that consists of two simulated neurons in mutual inhibition. The adjacent two CPGs are coupled, and the CPG model^{16,17} is shown in Fig. 3.

Hence, the CPG model can be described by

$$\left. \begin{aligned} T_r \dot{u}_i^f + u_i^f &= -bv_i^f - wg(u_i^e) - \sum w_{ij}y_j + c \\ T_a \dot{v}_i^f + v_i^f &= g(u_i^f) \\ T_r \dot{u}_i^e + u_i^e &= -bv_i^e - wg(u_i^f) - \sum w_{ij}y_j + c \\ T_a \dot{v}_i^e + v_i^e &= g(u_i^e) \\ y_i &= g(u_i^f) - g(u_i^e) \end{aligned} \right\}. \tag{1}$$

Function $g(\bullet)$ is a piecewise linear function defined by $g(x) = \max(o,x)$, which represents a threshold property of the neurons. Variables u_i^f , u_i^e , and y_i represent the membrane potential and the firing rate of the neurons, respectively. Two variables v_i^f and v_i^e represent the adaptations or fatigue properties that ubiquitously exist in real neurons. Parameter c denotes the tonic input, and parameter w_{ij} is the strength of mutual inhibition from neuron i to j . Parameters w and b represent the strength of mutual and self-inhibition, respectively. Parameters T_r and T_a are the time constants that determine the reaction times of variables u_i^f , u_i^e and v_i^f , v_i^e .

In this model, the neurons are coupled to one another in a depressive manner, and the entire walking behavior undergoes an adaptation process by causing an oscillation in each joint movement. The movement of a joint is coupled with that of other joint. The entire walking behavior converges

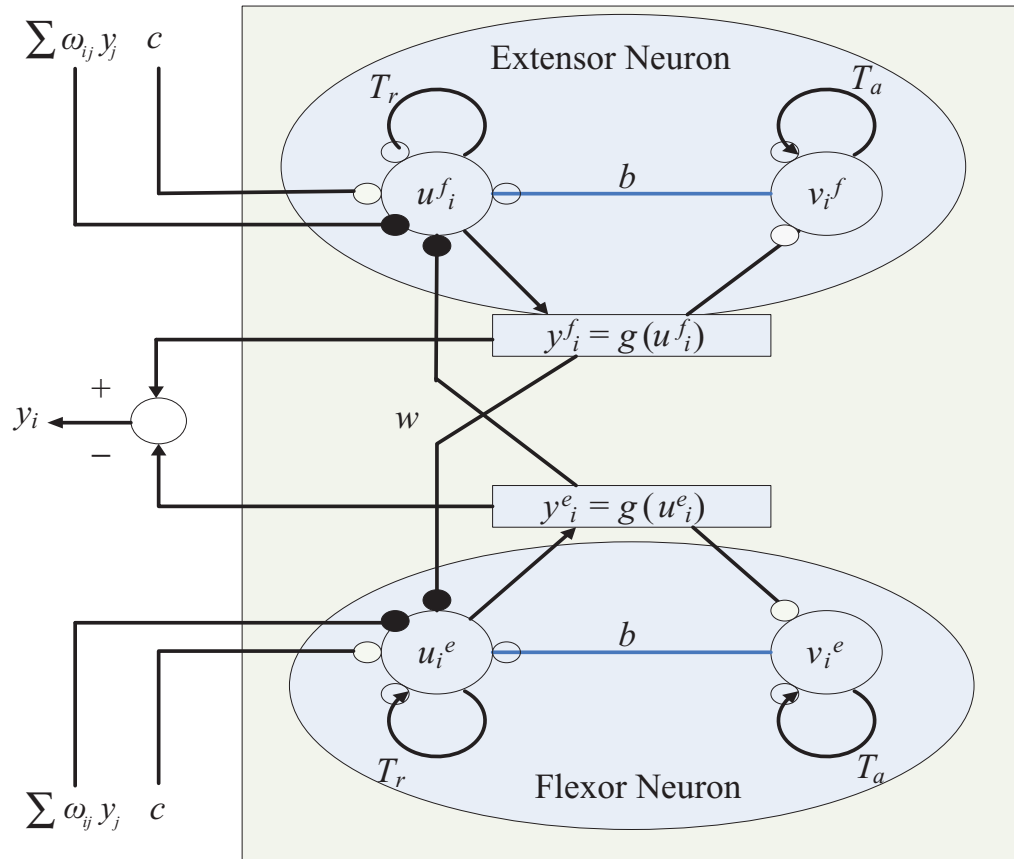


Fig. 3. The CPG model.

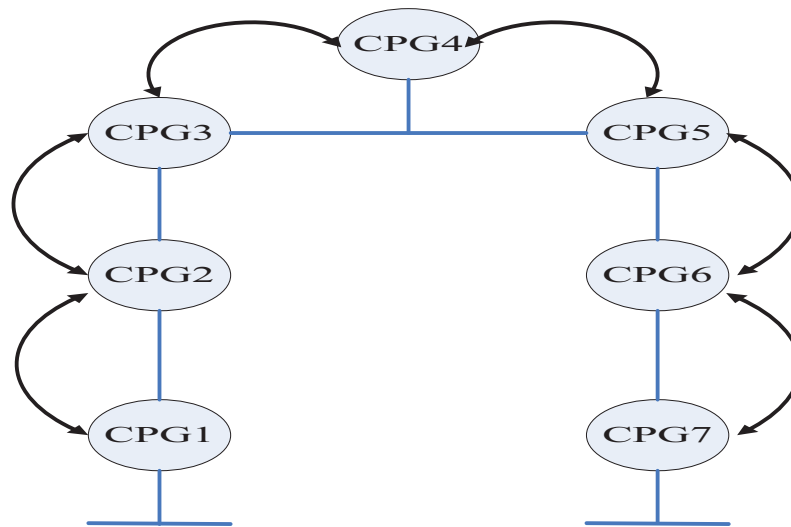


Fig. 4. The CPG network.

to a certain stable walking pattern in a harmonious manner through the adaptation process of an oscillator.

Based on the CPG model given in Fig. 3, the CPG network, i.e., the arrangement of CPGs in the biped robot,¹⁸ is shown in Fig. 4.

The topology of the CPG network is annular. These adjacent CPGs are coupled to one another with different values of joint angles. The new CPG network can be described by

$$\left\{ \begin{array}{l} T_r \dot{x}_1 + x_1 = -bx_8 - w \max(0, x_2) + c \\ T_a \dot{x}_8 + x_8 = \max(0, x_1) \\ T_r \dot{x}_2 + x_2 = -bx_9 - w \max(0, x_1) - w \max(0, x_3) + c \\ T_a \dot{x}_9 + x_9 = \max(0, x_2) \\ T_r \dot{x}_3 + x_3 = -bx_{10} - w \max(0, x_2) - w \max(0, x_4) + c \\ T_a \dot{x}_{10} + x_{10} = \max(0, x_3) \\ T_r \dot{x}_4 + x_4 = -bx_{11} - w \max(0, x_3) - w \max(0, x_5) + c \\ T_a \dot{x}_{11} + x_{11} = \max(0, x_4) \\ T_r \dot{x}_5 + x_5 = -bx_{12} - w \max(0, x_4) - w \max(0, x_6) + c \\ T_a \dot{x}_{12} + x_{12} = \max(0, x_5) \\ T_r \dot{x}_6 + x_6 = -bx_{13} - w \max(0, x_5) - w \max(0, x_7) + c \\ T_a \dot{x}_{13} + x_{13} = \max(0, x_6) \\ T_r \dot{x}_7 + x_7 = -bx_{14} - w \max(0, x_6) + c \\ T_a \dot{x}_{14} + x_{14} = \max(0, x_7) \\ \text{theta1} = \max(0, x_1) - \max(0, x_2) \\ \text{theta2} = \max(0, x_2) - \max(0, x_3) \\ \text{theta3} = \max(0, x_3) - \max(0, x_4) \\ \text{theta4} = \max(0, x_4) - \max(0, x_5) \\ \text{theta5} = \max(0, x_5) - \max(0, x_6) \\ \text{theta6} = \max(0, x_6) - \max(0, x_7) \end{array} \right. , \quad (2)$$

where $w_{ij} = w$, and theta1 , theta2 , theta3 , theta4 , theta5 , and theta6 are the outputs of these six joints, respectively. These variables $x_i (i = 1, \dots, 7)$ and $x_i (i = 8, \dots, 14)$ represent the membrane potentials and the self-inhibitory inputs respectively.

The maximal Lyapunov exponent (MLE) describes the time asymptotic rate of separation of infinitesimally close trajectories. A positive MLE is usually taken as an indication that the system is chaotic. The zero MLE indicates that a limit cycle exists in the system. The Lyapunov exponents of a stable fixed point are all negative. The diagrams of the Lyapunov exponents of CPGs' outputs are shown in Fig. 5 with $Tr = 0.1$ and $Ta = 1$, and the initial input values are $[0, 0, 0.1, 0, 0, 0, 0, 0, 0, 0.1, 0, 0.1, 0.1]$. Parameters b, c, w are varied in the interval $[1, 100]$ in step of 0.5. In Fig. 5(a), the MLEs of CPGs' outputs are zero for $b \in [3.5, 11], [12, 18.5], [19.5, 26.5]$, suggesting that the states of CPGs' outputs are limit cycles. Otherwise, the MLEs are negative or positive, suggesting that the states of CPGs' outputs are stable or chaotic. In Fig. 5(b), the MLEs of CPGs' outputs are zero for $c \in [2, 100]$, which means that the states of CPGs' outputs are limit cycles. Otherwise, the MLEs are negative, indicating that the states of the CPGs' outputs are stable. In Fig. 5(c), the MLEs of CPGs' outputs are zero for $w \in [1, 1.5]$, which means that the states of CPGs' outputs are limit cycles. Otherwise, the MLEs are negative or positive, indicating that the states of the CPGs' outputs are stable or chaotic.

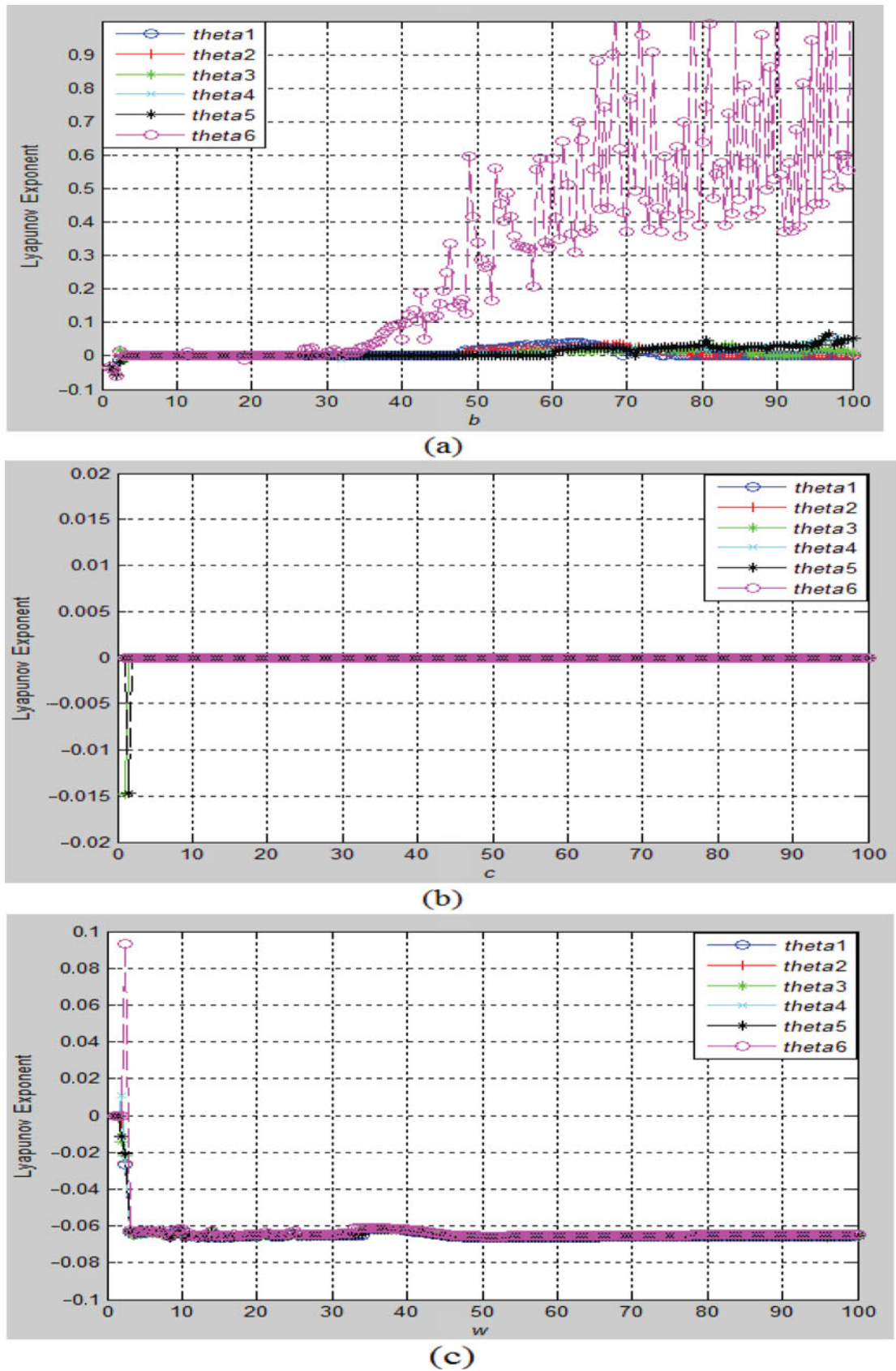


Fig. 5. Lyapunov exponent diagrams of CPGs' outputs with parameters b , c , w . (a) $b \in [1, 100]$. (b) $c \in [1, 100]$. (c) $w \in [1, 100]$.

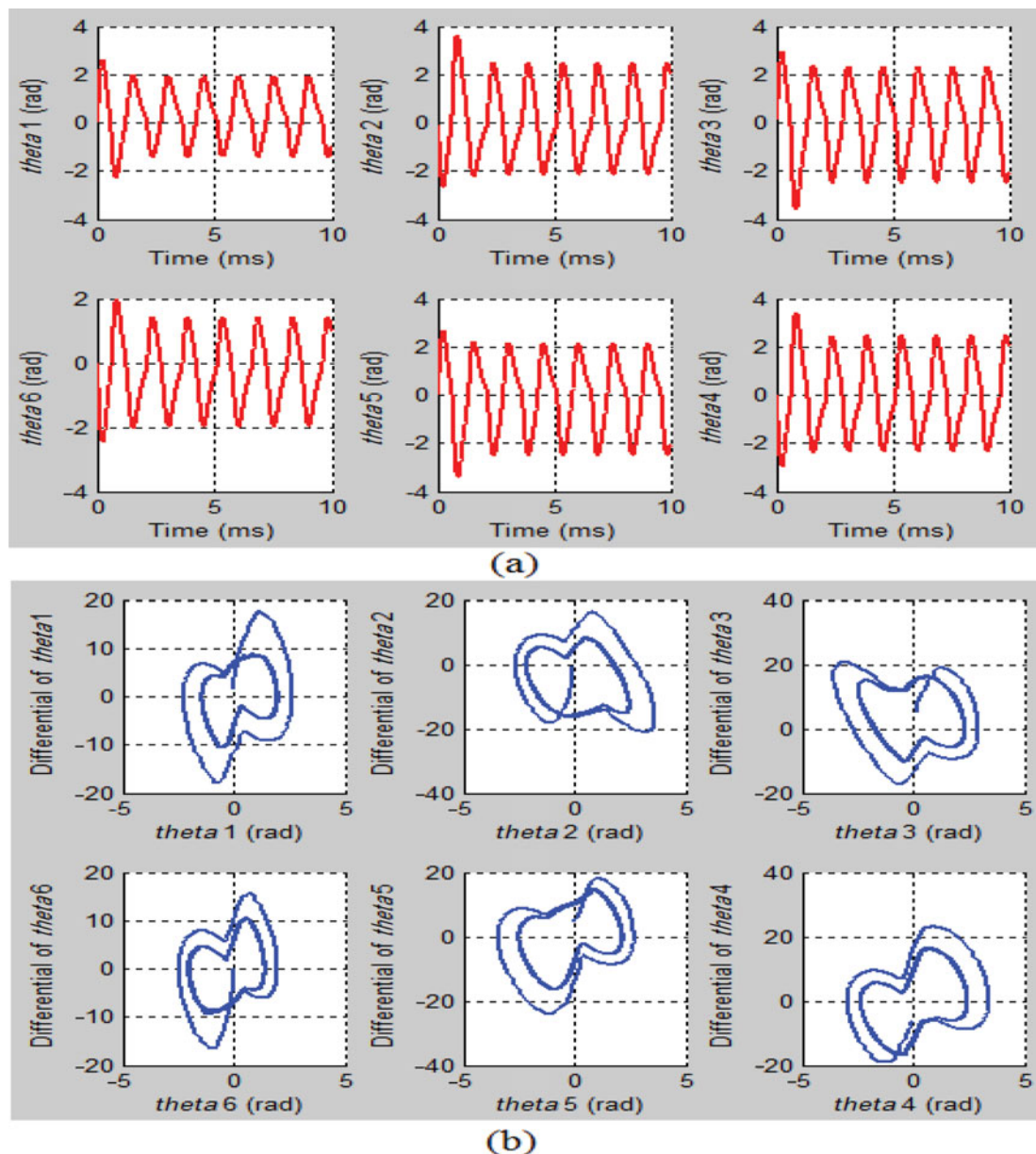


Fig. 6. Outputs and phase diagrams of CPGs. (a) Outputs of CPGs. (b) Phase diagrams of CPGs.

In this paper, the states of CPGs' outputs are expected to be limit cycles. Based on the above analysis, the three parameters b , c , and w are set as $b = 4.5$, $c = 2$, and $w = 1.5$ respectively. All the outputs and phase diagrams of CPGs are shown in Fig. 6.

In Fig. 6, θ_1 and θ_6 , θ_2 and θ_5 , and θ_3 and θ_4 have better performance of phase complementarity. Every phase diagram is a stable limit cycle.

2.3. Evaluation of robustness

In order to confirm the robustness of a CPG network against disturbance, the external interference¹⁹ is described by

$$z = A \sin \left(2\pi \times \frac{x}{\lambda} \right). \quad (3)$$

Here λ and A are the period and amplitude of external interference respectively.

Figure 7 shows the limit cycle of these six joint angles when the external interferences are set to (a) $\lambda = 20$ cm and $A = 0.5$ cm, or (b) $\lambda = 20$ cm and $A = 4$ cm. As the amplitude increases, the

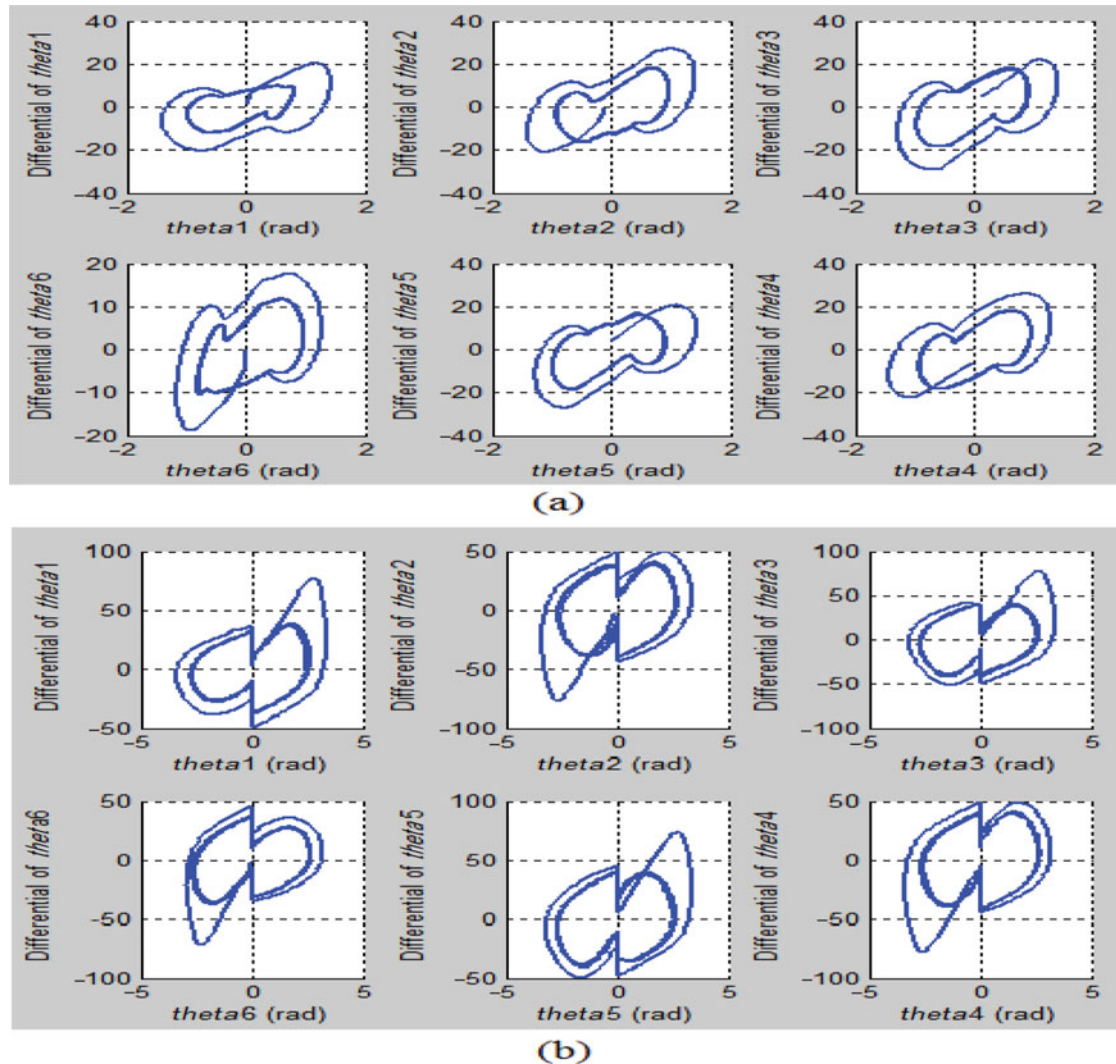


Fig. 7. Phase diagrams with (a) $\lambda = 20$ cm, $A = 0.5$ cm, and (b) $\lambda = 20$ cm, $A = 4$ cm.

deviation from the limit cycle also increases. In Fig. 7(b), these six joint angles deviate largely from the limit cycle and finally fall to their stable state. The results show that the CPG network has high robust performance.

3. Model of Central Nervous System

The neural network provides a robust approach to the approximation of target functions. The artificial neural networks that can learn to interpret complex real-world sensor data are the most effective learning methods currently known.¹⁷ In this paper, the Radial Basis Function (RBF) neural network is employed to imitate the cerebral cortex. A typical RBF neural network has a three-layer feed-forward structure that can be trained to learn an input–output relationship based on a data set.²⁰ The structure of RBF neural network is shown in Fig. 8.

In general, the RBF neural network can be applied to solve all kinds of nonlinear problems because the mapping relationship between the input and output is nonlinear. Compared with any other kind of neural network, the RBF neural network is featured with simple network structure, fast convergence rate, and strong approximation ability.²¹

In this paper, we use the neural network to predict the CPG network parameter values that correspond to the next gait. The neural network should adapt itself to fast gait transition with fast convergence rate. Therefore, the RBF neural network is chosen to simulate the cerebral cortex. To

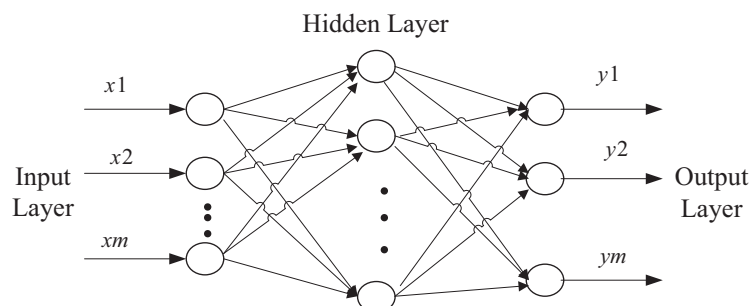


Fig. 8. Structure of an RBF neural network.

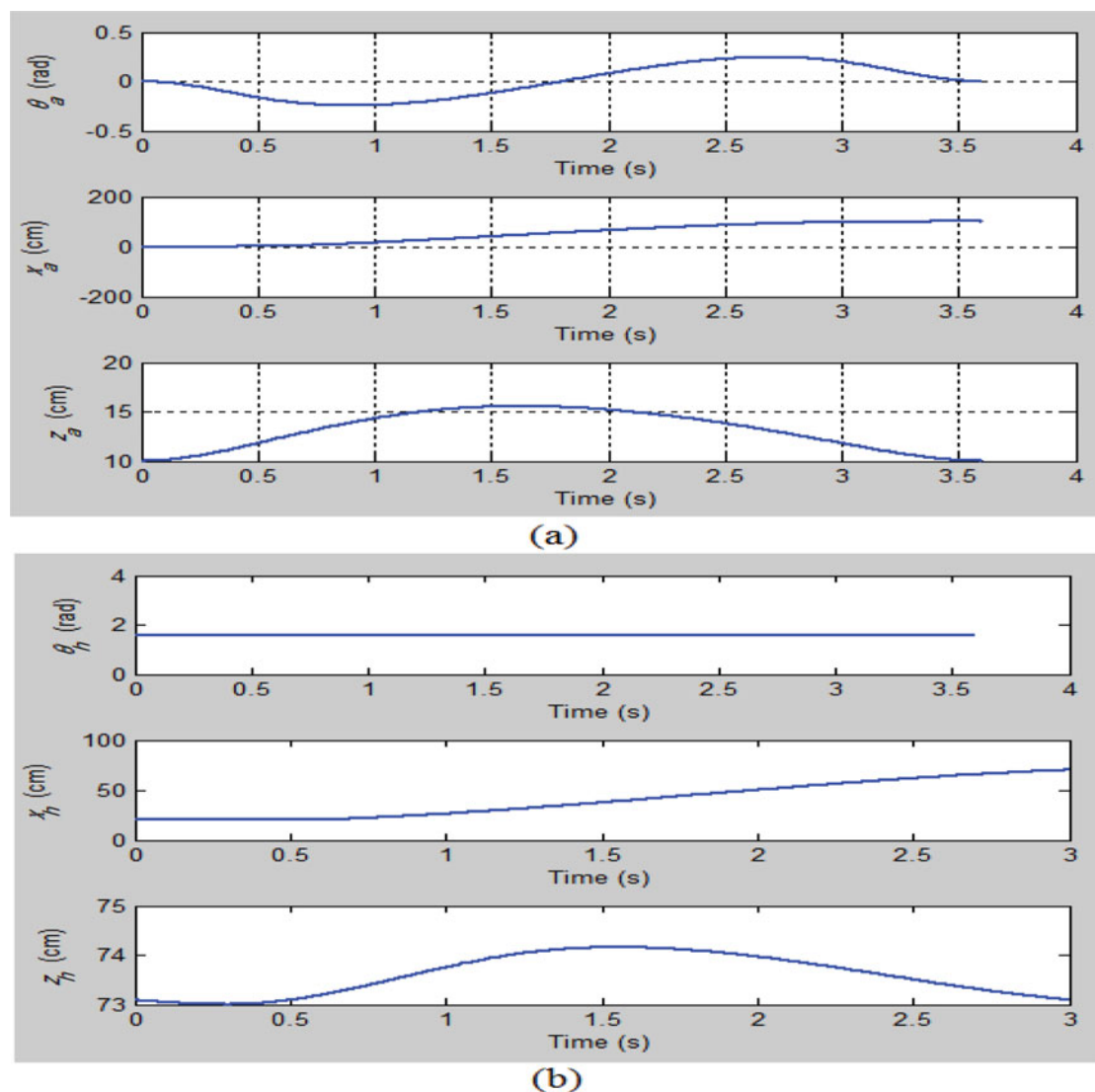


Fig. 9. Curves of robot's ankle and hip. (a) Curve of robot's ankle. (b) Curve of robot's hip.

the RBF neural network, the inputs are environmental change and the time series of the current gait. The outputs are the parameter c and the time series of the next gait.

In Fig. 1, a pattern mapping is needed to transform the outputs of a CPG network to positions and angles that inspire the musculoskeletal system. The Credit-Assignment Cerebellar Model Articulation Controller (CA-CMAC) algorithm is adopted to realize this conversion.

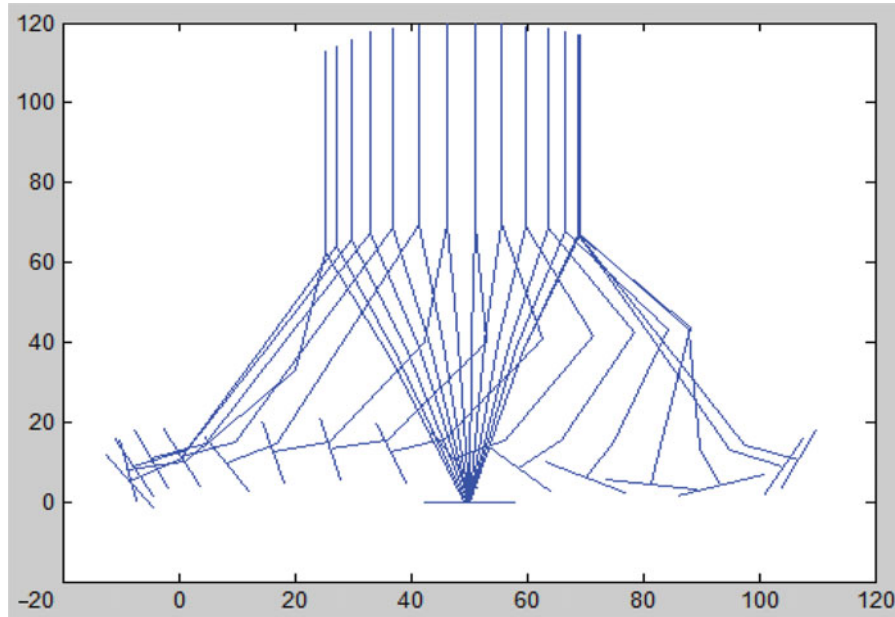


Fig. 10. Stick figure of the walking movement based on the planning.

The CA-CMAC²² can be considered as an associative memory network, and it performs two subsequent mappings: $f : X \rightarrow A$, $h : A \rightarrow P$, where X is M -dimension input space, A is an N -dimension association cell vector, and P is one-dimension output space. The output is shown in Eq. (4),

$$y_s = \sum_{j=1}^N C_s \omega_j, \quad (4)$$

where N is the number of memory elements, y_s is the output of state s , ω_j is the weight of the j th memory element, and C_s is the flag whether the j th memory element is activated. If activated, the value is 1, otherwise the value is 0. The update rule to the weights is described by

$$\omega_j^i = \omega_j^{i-1} + \alpha C_s \left\{ \frac{(f(j) + 1)^{-1}}{\sum_{l=1}^m (f(l) + 1)^{-1}} \right\} \times \left(\bar{y}_s - \sum_{j=1}^N C_s \omega_j^{i-1} \right), \quad (5)$$

where α is the learning rate, and $f(j)$ is the activated times of the j th memory cell.

In comparison with other algorithms, CA-CMAC has the advantage of very fast learning and it has a unique property of quickly training certain areas of memory without affecting the whole memory structure. The advantage of speed in training is very important in fast gait transition, and the local generalization is particularly suitable for local area features' conversion.²³

4. Simulations and Results

4.1. Simulation scheme

Simulation is conducted to verify the proposed locomotion model. The walking gait is planned,¹⁵ and the angles of planning gait corresponding to periodic oscillations are generated by the CPG network. In this simulation, the environmental change is supposed to be the height of the obstacle, which is proportional to the amplitude of the CPG network. Matsuoka²⁴ showed that the amplitude of the CPG network is proportional to the tonic input c if other parameters are fixed. The relation is described by

$$A_x = \frac{c}{\frac{2(T_r+T_a)}{T_a w} - 1 + \frac{2}{\pi}(w+b) \sin^{-1} \left(\frac{T_r+T_a}{T_a w} \right)}, \quad (6)$$

where A_x is the amplitude.

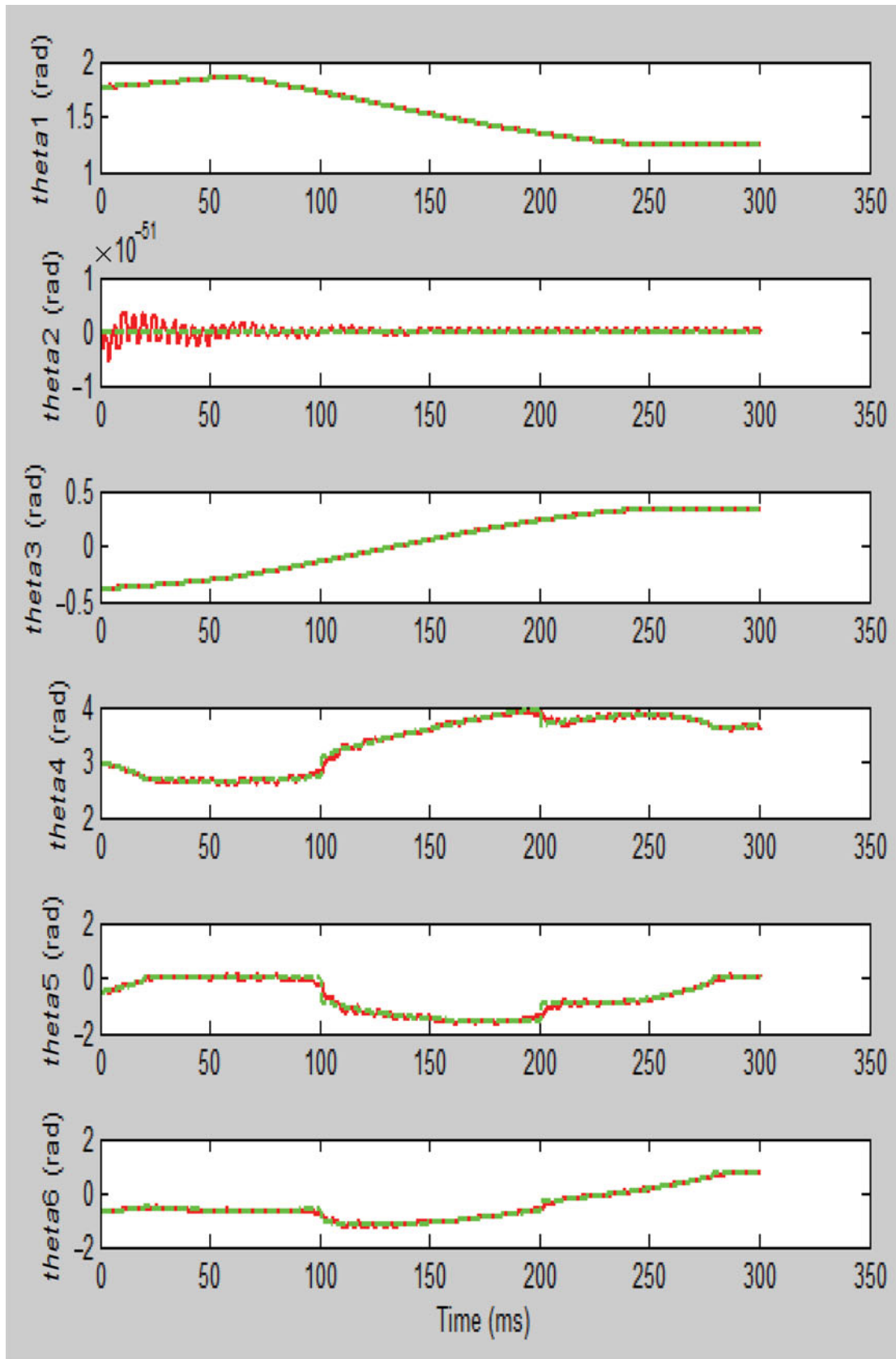


Fig. 11. Fitting curves between the planning and output angles.

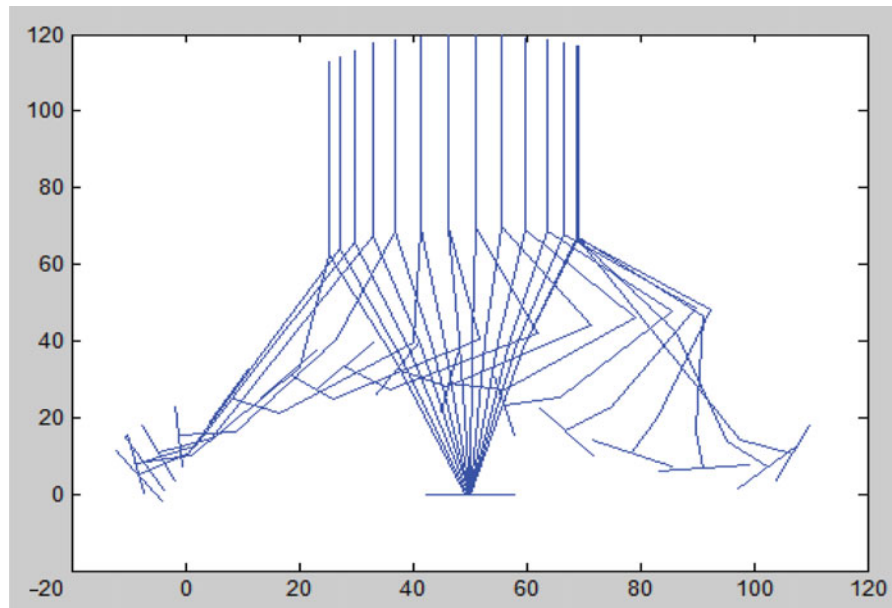


Fig. 12. Stick figure of the walking movement.

Therefore, the environmental change is proportional to the parameter c . In the locomotion model, the cerebral cortex predicts the value of parameter c , which corresponds to the next gait according to the environmental change and current gait. The cerebellum calculates the mean square deviation of a cycle oscillation, which is treated as compensation.

Many scientific researchers have used the stick figure to demonstrate their studies.^{15,25–27} Therefore, the stick figure is also used to simulate the locomotion model in this paper.

4.2. Simulation

The parameters are set as $T_c = 3$ s, $T_d = 0.6$ s, $q_b = 0.2$ rad, $q_f = 0.2$ rad, $D_s = 50$ cm, $T_m = 1.2$ s, $L_{ao} = 25$ cm, $H_{ao} = 15$ cm, $H_{hmin} = 73$ cm, $H_{hmax} = 74$ cm, $x_{ed} = 20$ cm, and $x_{sd} = 30$ cm. From the viewpoint of stability, we assume that the hip motion parameter $\theta_h(t)$ is constant when there is no waist joint; in particular, $\theta_h(t) = 0.5\pi$ rad on level ground.¹⁵ Then the curves of the robot's ankle and hip are obtained, as shown in Fig. 9.

According to the planning and kinetics, the stick figure of the walking movement is obtained as shown in Fig. 10.

During the training of an RBF neural network, the environmental value is developed from 0 to 10 cm and the step is 0.1. The value of the corresponding parameter c is changed from 15 to 25 and the step is also 0.1. The sampling numbers of CPG are 300. In the walking gait planning, the value of parameter H_{ao} is changed from 15 to 25 cm. These six joint angles are needed to be converted in this simulation. Hence, the six parallel CA-CMACs are chosen to realize the pattern mapping for $N = 5$ in Eq. (4) and $\alpha = 0.2$ in Eq. (5). In the simulation, the initial value of H_{ao} is 15 cm and it is changed to 25 cm. According to the simulation scheme, the fitting curves between the planning angles and the output angles based on CA-CMAC are obtained in Fig. 11, and the stick figure of the walking movement is expressed in Fig. 12.

Comparing Fig. 10 with Fig. 12, the cerebral cortex can adjust the value of parameter c when the environmental value is changed from 0 to 10 cm. Hence, the robot can avoid the obstacle in its moving course. From the simulation results, we can see that the outputs of a CPG network can be treated as proprioception that provides the central nervous system with the information about all joints' angles. Therefore, we can draw a conclusion that the cerebral cortex can modulate the CPG parameters to adjust the walking gait.

5. Conclusions

In the present study, we focused on the human locomotion model and the CPG network. The CPG network outputs treated as the proprioception cannot only inspire the musculoskeletal system to

obtain natural gait but also be a feedback to the central nervous system to modulate the walking gait of robot. Here we only discuss the coupling effect between the CPG network and the central nervous system. Their complex dynamic characters deserve further investigation.

Acknowledgements

The work was supported by National Natural Science Foundation of China under grants 61040056 and 61070127, Shanghai Key Project of Foundation funding under grant 09JC1414600, China, and Huo Yingdong Foundation for basic research under grant 121064, China.

References

1. K. Matsuoka, "Sustained oscillations generated by mutually inhibiting neurons with adaptation," *Biol. Cybern.* **52**(6), 367–376 (1985).
2. C. Fu, F. Tan and K. Chen, "A simple walking strategy for biped walking based on an intermittent sinusoidal oscillator," *Robotica* **28**(6), 869–884 (2010).
3. G. Liu, M. K. Habib, K. Watanabe and K. Izumi, "Central pattern generators based on Matsuoka oscillators for the locomotion of biped robots," *Artif. Life Robot.* **12**, 264–269 (2008).
4. T. Ha and C. H. Choi, "An effective trajectory generation method for bipedal walking," *Robot. Auton. Syst.* **55**, 795–810 (2007).
5. X. Zhang and H. Zheng, "Autonomously clearing obstacles using the biological flexor reflex in a quadrupedal robot," *Robotica* **26**, 1–7 (2008).
6. T. Kondo and K. Ito, "Periodic Motion Control by Modulating CPG Parameters Based on Time-Series Recognition," *Proceedings of the 8th European Conference on Artificial Life*, Canterbury, UK (2005) pp. 906–915.
7. H. H. Ehrsson, C. Spence and R. E. Passingham, "'That's my hand!' Activity in the premotor cortex reflects feeling of ownership of a limb," *Science* **305**, 875–877 (2004).
8. H. H. Ehrsson, "The experimental induction of out-of-body experiences," *Science* **317**, 1048 (2007).
9. J. L. Overholt, G. R. Hudas and G. R. Gerhart, "Defining Proprioceptive Behaviors for Autonomous Mobile Robots," *Proceedings of SPIE*, Orlando, FL (2002) pp. 287–294.
10. R. J. van Beers, A. C. Sittig and J. J. D. van der Gon, "The precision of proprioceptive position sense," *Exp. Brain Res.* **122**, 367–377 (1998).
11. S. Bartsch and F. Kirchner, "Robust Control of a Humanoid Robot Using a Bio-Inspired Approach Based on Central Pattern Generators, Reflexes, and Proprioceptive Feedback," *IEEE International Conference on Robotics and Biomimetics*, Kunming, China (2006) pp. 1547–1552.
12. T. Drew, S. Prentice and B. Schepens, "Cortical and brainstem control of locomotion," *Prog. Brain Res.* **143**, 251–261 (2004).
13. K. Takakusaki and T. Okumura, "Neurobiological basis of controlling posture and locomotion," *Adv. Robot.* **22**, 1629–1663 (2008).
14. G. Taga, "A model of the neuro-musculo-skeletal system for human locomotion. I. Emergence of basic gait," *Biol. Cybern.* **73**, 97–111 (1995).
15. Q. Huang, K. Yokoi and S. Kajita, "Planning walking patterns for a biped robot," *IEEE Trans. Robot. Autom.* **17**(3), 280–289 (2001).
16. Y. Fukuoka, H. Kimura and A. H. Cohen, "Adaptive dynamic walking of a quadruped robot on irregular terrain based on biological concepts," *Int. J. Robot. Res.* **22**, 187–203 (2003).
17. X. Zhang, Biological-Inspired Rhythmic Motion & Environmental Adaptability for Quadruped Robot, *PhD Dissertation*, Department Of Mechanical Engineering, Tsinghua University, Beijing, China (2004) pp. 41–62.
18. J. J. Kim, J. W. Lee and J. J. Lee, "Central pattern generator parameter search for a biped walking robot using nonparametric estimation based particles swarm optimization," *Int. J. Control Autom. Syst.* **7**(3), 447–457 (2009).
19. Y. Kim, Y. Tagawa, G. Obinata and K. Hase, "Robust control of CPG-based 3D neuromusculoskeletal walking model," *Biol. Cybern.* **105**, 269–282 (2011).
20. W. E. Wong, V. Debroy, R. Golden, X. Xu and B. Thuraisingham, "Effective software fault localization using an RBF neural network," *IEEE Trans. Reliab.* **61**(1), 149–169 (2012).
21. X. Wu, G. Jiang, X. Wang, N. Fang, L. Zhao, Y. Ma and S. Luo, "Prediction of reservoir sensitivity using RBF neural network with trainable radial basis function," *Neural Comput. Appl.* **22**, 947–953 (2013).
22. S. F. Su, T. Tao and T. H. Hung, "Credit-assigned CMAC and its application to online learning robust controllers," *IEEE Trans. Syst. Man Cybern. B* **33**(2), 202–213 (2003).
23. Y. Wang, Y. Tao, B. Nie, and H. Liu, "Optimal design of control for scan tracking measurement: A CMAC approach," *Measurement* **46**, 384–392 (2013).
24. K. Matsuoka, "Analysis of a neural oscillator," *Biol. Cybern.* **104**, 297–304 (2011).

25. C. Liu, C. G. Atkeson and J. Su, "Biped walking control using a trajectory library," *Robotica* **31**(2), 311–322 (2013).
26. G. Bessonnet, S. Chesse and P. Sardain, "Optimal gait synthesis of a seven-link planar biped," *Int. J. Robot. Res.* **23**(10–11), 1059–1073 (2004).
27. M. Ishida, S. Kato, M. Kanoh and H. Itoh, "Generating Locomotion for Biped Robots Based on the Dynamic Passivization of Joint Control," *Proceedings of the 2009 IEEE International Conference on Systems, Man, and Cybernetics*, San Antonio, TX (2009) pp. 3157–3162.